Molecular Cancer Therapeutics

Ibrutinib Inhibits ERBB Receptor Tyrosine Kinases and HER2-Amplified Breast Cancer Cell Growth

Jun Chen[1], Taisei Kinoshita[1], Juthamas Sukbuntherng[2], Betty Y. Chang[1], and Laurence Elias[1]

Abstract

Ibrutinib is a potent, small-molecule Bruton tyrosine kinase (BTK) inhibitor developed for the treatment of B-cell malignancies. Ibrutinib covalently binds to Cys481 in the ATP-binding domain of BTK. This cysteine residue is conserved among 9 other tyrosine kinases, including HER2 and EGFR, which can be targeted. Screening large panels of cell lines demonstrated that ibrutinib was growth inhibitory against some solid tumor cells, including those inhibited by other HER2/EGFR inhibitors. Among sensitive cell lines, breast cancer lines with HER2 overexpression were most potently inhibited by ibrutinib (<100 nmol/L); in addition, the IC_{50}s were lower than that of lapatinib and dacomitinib. Inhibition of cell growth by ibrutinib coincided with downregulation of phosphorylation on HER2 and EGFR and their downstream targets, AKT and ERK. Irreversible inhibition of HER2 and EGFR in breast cancer cells was established after 30-minute incubation above 100 nmol/L or following 2-hour incubation at lower concentrations. Furthermore, ibrutinib inhibited recombinant HER2 and EGFR activity that was resistant to dialysis and rapid dilution, suggesting an irreversible interaction. The dual activity toward TEC family (BTK and ITK) and ERBB family kinases was unique to ibrutinib, as ERBB inhibitors do not inhibit or covalently bind BTK or ITK. Xenograft studies with $HER2^+$ MDA-MB-453 and BT-474 cells in mice in conjunction with determination of pharmacokinetics demonstrated significant exposure-dependent inhibition of growth and key signaling molecules at levels that are clinically achievable. Ibrutinib's unique dual spectrum of activity against both TEC family and ERBB kinases suggests broader applications of ibrutinib in oncology. *Mol Cancer Ther; 15(12); 2835–44. ©2016 AACR.*

Introduction

Ibrutinib is a tyrosine kinase inhibitor (TKI) designed primarily to target Bruton tyrosine kinase (BTK), which is expressed predominantly in the B-lymphocytic and myelomonocytic lineages (1). Ibrutinib has shown notable clinical activity against several B-cell lymphoproliferative diseases, especially chronic lymphocytic leukemia (CLL), mantle cell lymphoma (MCL), and Waldenström macroglobulinemia (2, 3). It binds covalently to Cys481 in the kinase domain of BTK and exhibits excellent selectivity, as only 9 other tyrosine kinases have the homologous cysteine residue (1). Rapid binding of ibrutinib to its target also leads to efficient inhibition of BTK without requiring sustained systemic exposure. This property of ibrutinib enables clinically effective and well tolerated once-a-day dosing despite its short plasma half-life in human subjects.

ERBB family kinases are among those kinases with homologous active site cysteines, specifically Cys797 in EGFR, Cys805 in ERBB2 (HER2), and Cys803 in ERBB4 (HER4), which have been known to be sensitive to ibrutinib in biochemical assays since its discovery (1). Grabinski and colleagues (4) recently reported that ibrutinib inhibited phosphorylation of EGFR, HER2, and HER3, as well as the downstream targets AKT and MAPK, leading to a reduction of cell viability at nanomolar concentrations in $HER2^+$ breast cancer cell lines. Antitumor effects of ibrutinib have also been reported in a subset of EGFR-driven non–small cell lung cancer (NSCLC) lines (5). Members of the ERBB family of tyrosine kinase receptors are frequently abnormal in structure or expression in many human cancers and have proven to be important therapeutic targets. For example, approximately 20% of breast cancers have genomic amplification of the *HER2* gene and are often treatable by HER2-targeted monoclonal antibodies (mAb) and TKIs. NSCLC frequently harbors activating mutations of EGFR that are targeted by a number of TKIs and mAbs (5, 6). Other cancer types, most notably gastric and gastroesophageal junction carcinoma, colorectal carcinomas, and head and neck carcinomas, share such abnormalities in subsets of patients and may be similarly treatable (7–9).

Several recently developed TKIs are capable of forming covalent bonds with the conserved cysteine in the ATP-binding pocket (10–14). Although TKIs are highly effective in targeting ERBB kinases, ibrutinib could have additional desirable effects in solid tumor settings based on its concurrent activity against TEC family kinases. Inhibition of IL2-inducible T-cell kinase (ITK) has been reported to modulate a Th cell population toward Th1, a subset of Th cells known to be important for T-cell–mediated antitumor immunity (15). Ibrutinib in combination with anti-PD-L1 antibody was shown to provoke strong host T-cell–mediated antitumor activity against various tumor types (16). Inhibition of BTK by ibrutinib has been suggested to be beneficial in some models by modulating myeloid-derived suppressor cells (17) and mast cells (18). Thus, if ibrutinib has clinically meaningful HER2-targeting activity, its effectiveness could be augmented by such

[1]Research Department, Pharmacyclics LLC, an AbbVie Company, Sunnyvale, California. [2]Clinical Pharmacology and DMPK Department, Pharmacyclics LLC, an AbbVie Company, Sunnyvale, California.

Note: Supplementary data for this article are available at Molecular Cancer Therapeutics Online (http://mct.aacrjournals.org/).

Corresponding Author: Betty Y. Chang, Pharmacyclics LLC, an AbbVie Company, 995 East Arques Avenue, Sunnyvale, CA 94085. Phone: 408-215-3358; Fax: 408-215-3358; E-mail: bchang@pcyc.com

doi: 10.1158/1535-7163.MCT-15-0923

modulation of the tumor microenvironment. In the current study, we sought to address several questions that have critical bearing on potential applicability of ibrutinib to HER2-overexpressing breast cancer: (i) how potent is ibrutinib in inhibiting these cells *in vitro* and *in vivo*, particularly compared with other approved or investigational ERBB kinase inhibitors? (ii) does ibrutinib bind irreversibly to these enzyme targets? (iii) can antitumor effects be anticipated at clinically attainable exposure levels? (iv) does ibrutinib have attributes that would be of distinguishing utility compared with other highly active ERBB family inhibitors? The evidence presented here indicates that ibrutinib is sufficiently potent and functions as an irreversible HER2 inhibitor at clinically attainable exposure levels while exhibiting notably greater activity against ITK or BTK than several ERBB family inhibitors tested.

Materials and Methods

Cell lines and inhibitors

All cell lines were directly obtained from the ATCC, except for SUM-185PE (Asterand) and MFM-223 (Sigma-Aldrich), between 2013 and 2014 and maintained in culture as recommended. A frozen stock was established immediately after receiving each cell line, and only early passage (<2 months) cells from the initially established frozen cell lines were used in the study. Cell lines were routinely tested for mycoplasma contamination. Ibrutinib (PCI-32765) and the fluorescein-labeled ibrutinib probe PCI-33380 (1) were synthesized at Pharmacyclics LLC. The ERBB family of inhibitors was obtained from Selleck Chemicals.

Growth inhibition experiments and apoptosis assays

Two panels of solid tumor cell lines, a 230-cancer cell panel and the NCI-60 panel, were screened for growth inhibitory activity by ibrutinib. These screens were performed at the Massachusetts General Hospital (Boston, MA) and National Cancer Institute (Bethesda, MD), respectively, as described previously (19, 20). Further *in vitro* growth inhibition experiments were performed by 72-hour treatment in duplicate or triplicate format with AlamarBlue (Invitrogen, Life Technologies) or CellTiter-Glo (Promega) assay. Cell apoptosis was assayed with Annexin-V/PI staining (BioVision) and flow cytometer (BD FACSCalibur) using the manufacturer's recommended methods. The pan-caspase inhibitor quinoline-Val-Asp(Ome)-CH2-O-phenoxy (Q-VD-OPh; MP Biomedicals) was used at 10 μmol/L to test the caspase dependence of apoptosis.

Xenograft tumor mouse models and pharmacokinetics/pharmacodynamics

Tumor growth inhibition was determined in CB17/SCID mice for MDA-MB-453 and NOD-SCID or BALB/c nude mice for BT-474. Cells were inoculated orthotopically in mouse mammary fat pads. Each group consisted of 10 animals or up to 21 when pharmacokinetic study was performed at the end of the study. Experiments using BT-474 models were conducted by Crown Bioscience (Santa Clara, CA). Ibrutinib was orally administered once daily after the tumor mass reached approximately 100 to 150 mm^3. Choice of doses was guided by prior experience with ibrutinib in a range of tumor models, with doses of approximately 12 to 16 mg/kg/d generally found to be effective and well tolerated, but not maximally inhibitory, and doses around 48 mg/kg/d to be more efficacious. Tumor was measured once each week with a vernier caliper for the MDA-MB-453 model and 2 or 3 times for the BT-474 model. The volume was calculated with the formula $width^2 \times length \times 0.4$ for MDA-MB-453 and $width^2 \times length \times 0.5$ for BT-474 tumors. Relative tumor growth inhibition was quantified by the ratio of the area under the curve (AUC) [1−(AUC ibrutinib/AUC vehicle)], which was calculated using Microsoft Excel from the tumor growth curve, with the baseline set at the time of initial dosing.

Pharmacokinetics was determined on plasma samples from efficacy studies (BT-474) at the end of the study or from a separate group of tumor-bearing mice (MDA-MB-453). Blood samples were collected at different time points from 3 to 4 mice for each time point. Ibrutinib levels were measured in plasma using high-performance liquid chromatography (HPLC) with tandem mass spectrometry (LC/MS-MS). Pharmacokinetic parameters were determined by noncompartmental methods using Phoenix WinNonlin version 6.3.0 (Certara USA, Inc) as described previously (1, 3).

The relationships between pharmacokinetics and pharmacodynamics were fitted to E_{max} model using Phoenix WinNonlin. The simple E_{max} model described pAKT inhibition well, whereas the sigmoid E_{max} model better described tumor growth inhibition data:

$$pAktInh = \frac{E_{MAX}AUC}{AUC_{50} + AUC}$$

and

$$TumorInh = \frac{E_{MAX}AUC^{\gamma}}{AUC_{50}^{\gamma} + AUC^{\gamma}}$$

where *pAktInh* and *TumorInh* are percentage inhibition of AKT phosphorylation from Western blot measurements and of tumor growth, and E_{max} and AUC_{50} denote the calculated maximal and half-maximal effect levels; γ is the hill coefficient. For MDA-MB-453 tumor, tumor inhibition values were obtained from initial dosing to day 28 postdosing, because spontaneous regression was observed after day 28.

Immunohistochemical analysis of BT-474 tumor samples

At the end of the xenograft study, half of the tumor from each mouse was snap frozen for Western blotting, and the other half was fixed in neutral-buffered formalin and processed for IHC. The staining was conducted by Bioscience Solutions Group (Concord, MA). Four-micron sections were incubated with primary antibody overnight at 4°C and secondary antibody (EnVision+ Kits, Dako) for 30 minutes at room temperature. The slides were incubated with DAB and counterstained with hematoxylin. They were then scanned by Aperio AT Turbo (Leica Biosystems) with a 20× objective. Antibodies for phospho-HER2 (Tyr1221/1222), phospho-AKT (Ser473), phospho-ERK1/2 (Thr202/Tyr204), and Ki-67 (D3B5) were from Cell Signaling Technology. Immunohistochemical analysis was performed by 3 persons blinded to the treatment, and similar results were achieved.

Western blot analysis

Cells were washed with ice-cold PBS and lysed directly in 1× sample buffer from Invitrogen. Cell lysates were electrophoresed on Invitrogen 4%–12% Bis-Tris gels. After transferring the proteins to polyvinylidene difluoride membrane, the blot was probed with antibodies, and imaged using the LI-COR Odyssey imaging

system (Lincoln, NE). Antibodies for pEGFR (Y1086), pHER2 (Y1248), HER2, pHER3 (Y1289), pPLC-γ2 (Y1217), pBtk (Y223), ERK, pAKT, and AKT were from Cell Signaling Technology (Danvers, MA); antibodies for EGFR, pHER4 (Y1056), HER4, and pERK were from Santa Cruz Biotechnology (Dallas, TX). Paired mouse and rabbit antibodies were used to probe the total and corresponding phosphorylated proteins on the same blot.

Cell-cycle analysis

After detaching the cells from plate with trypsin-EDTA, they were fixed in 70% ethanol and stained with propidium iodide (PI)/RNase. PI staining in each cell was acquired with FACSCalibur, and data were analyzed using FlowJo software (Tree Star, Inc.).

BTK occupancy assay

The assay using the BODIPY-FL fluorophore–tagged ibrutinib congener PCI-33380 was performed as published previously (1).

Kinase assays and the irreversibility assays

In vitro kinase assays to quantify the potency of ibrutinib and other TKIs were performed on the LabChip platform by Nanosyn (Santa Clara, CA). Recombinant enzymes of ITK and HER4 were from Carna Bio (Natick, MA), EGFR and BTK from EMD Millipore, and HER2 and EGFR mutants from BPS Biosciences (San Diego, CA), Invitrogen, and Carna Bio.

Irreversibility of kinase inhibition was first assessed by dialysis assay following preincubation for 1 hour with test compounds at 0.1 and 0.01 μmol/L. After 24-hour dialysis, enzyme activity was measured in real-time format and initial velocity was determined. Undialyzed samples with compound were assembled similarly and preincubated for 1 hour. Their reversibility was also assessed by rapid dilution assay. The test compounds at 0.1 μmol/L were preincubated with each kinase for varying times between 5 and 90 minutes. The compound/kinase complexes were then rapidly diluted (dilution factor 1/500) into assay buffer followed by real-time enzyme activity assay. The initial velocity of the reaction was plotted against preincubation time to determine the apparent k_{obs} of inhibition.

Statistical analysis

Data were presented as mean ± SD for *in vitro* studies and mean ± SE for animal studies. The Student *t* test was used to assess the significance of the difference between the two means. CalcuSyn software (Biosoft, Great Shelford, Cambridge, United Kingdom) was used to calculate GI_{50}. Body weight and tumor volume were evaluated using a one-way ANOVA followed by Dunnett multiple comparison test when the initial analysis indicated that the means differed significantly ($P \leq 0.05$).

Results

Ibrutinib inhibits growth and key signaling pathways in HER2$^+$ breast cancer cell lines

High-throughput screening of ibrutinib for growth inhibitory activity against two panels of tumor cell lines, a 230-cancer cell panel and the NCI-60 panel (Supplementary Table S1), clearly indicated antiproliferative activity for certain solid tumor lines, and the profile in the NCI-60 panel showed significant qualitative similarities to the published patterns of two known EGFR inhibitors, gefitinib and lapatinib (20). The larger panel identified several other moderately sensitive carcinoma cell lines, with $IC_{50} \leq 100$ nmol/L, also in a general pattern consistent with EGFR and/or HER2 inhibition (data not shown). We further noted that sensitivity among lung cancer lines was usually restricted to cell lines with nonmutated *K-ras* gene, whereas all cell lines with activating mutations of *K-ras* had IC_{50} >1 μmol/L (Supplementary Table S2). BT-474, a breast cancer cell line, was found to have the highest sensitivity in the screening panels and in subsequent confirmatory experiments. We additionally tested several other breast cancer lines and found that MDA-MB-453, SK-BR-3, and UACC-893 also were sensitive, with $IC_{50} < 100$ nmol/L (Fig. 1A). These cell lines have all been well characterized as HER2-dependent for their proliferation (14, 21, 22). In contrast, other breast cancer cell lines with no HER2 amplification had little or no sensitivity to ibrutinib (Fig. 1B). Specifics of two cell lines, however, deserve comment. MDA-MB-361, although having HER2 amplification, was insensitive to ibrutinib. This cell line is an estrogen and progesterone receptor–expressing luminal A cell line and carries PI3K-activating mutation (23, 24). It was thus highly sensitive to a dual PI3K/mTOR inhibitor BEZ235 but not fulvestrant or temsirolimus (Supplementary Fig. S1). MDA-MB-468 was insensitive in our hands, despite being sensitive in the NCI-60 cell screen. This cell line is known for high genomic instability (25, 26) and has been reported as EGFR-overexpressing as well as frankly triple-negative by some investigators. Sensitivity of this line to lapatinib has been found to be markedly lower than that of other more typically HER2-overexpressing cell lines (27). NCI maintains an independent cell bank of NCI-60 lines, and it is also conceivable that some divergences emerged early in this line's passage history (20).

The observed pattern of sensitivity suggested that the mechanism of action by ibrutinib is through HER2 inhibition, so we have focused our further work on these cell lines. Ibrutinib inhibited HER2 and EGFR phosphorylation and downstream signaling in such breast cancer cells at concentrations comparable with those required for growth inhibition (Fig. 1A and C and Supplementary Fig. S2). The growth inhibition was manifested by G_1 arrest (Fig. 1D), and increasing proportions of apoptotic cells were detected with increased drug concentration, which were caspase-dependent (Fig. 1E). These observations are consistent with reported activity of other known HER2 inhibitors. Sensitive cell lines generally had higher basal levels of pAKT (Fig. 1F and Supplementary Fig. S3), which along with MEK-ERK phosphorylation was inhibited by ibrutinib. Although levels of pHER2 detectable by Western blot analysis appeared relatively low in MDA-MB-453 cells, the overall patterns of response of these cells were not atypical. HER2 and HER4 activation by heregulin β1 made cells less responsive to ibrutinib similarly in both MB-453 and BT-474 regarding signaling (Fig. 1G), as was cell growth (Fig. 1H). Compared with its potency against other common ERBB kinase inhibitors, ibrutinib was less potent than afatinib and neratinib but more potent than lapatinib, dacomitinib, and gefitinib in both BT-474 and SK-BR-3 cells (Supplementary Fig. S2). These comparisons were also examined in enzymatic assays (Table 1) wherein relative HER2-inhibitory activities were consistent with what was noted in cells. The inhibitory activity of lapatinib for HER2 was lower, whereas that for HER4 was higher than reported elsewhere (28), perhaps reflecting methodologic differences.

Ibrutinib suppresses growth of HER2$^+$ human breast cancer cells in xenograft models

We next conducted a series of xenograft studies with two tumorigenic HER2$^+$ cell lines, BT-474 and MDA-MB-453. In the

first study, treatment of BT-474 in NOD-SCID mice with ibrutinib at 16 mg/kg/d demonstrated modest yet significant impact on tumor growth, whereas the effect of the lower dose level was negligible (Supplementary Fig. S4A). Thus, higher doses were tested in the following experiments.

Because NOD-SCID mice did not tolerate ibrutinib at doses higher than 16 mg/kg per day, further BT-474 xenograft studies were performed in BALB/c nude mice, which had better tolerance. Ibrutinib at 16 and 48 mg/kg per day slowed tumor growth in this model, with a slight indication of dose dependence (Fig. 2A), and the reduction of tumor volume was 30% to 35% based on tumor volume AUC compared with the vehicle group. However, ibrutinib was more effective in the MDA-MB-453 xenograft model in CB17/SCID mice (Fig. 2B). In this model, ibrutinib exhibited

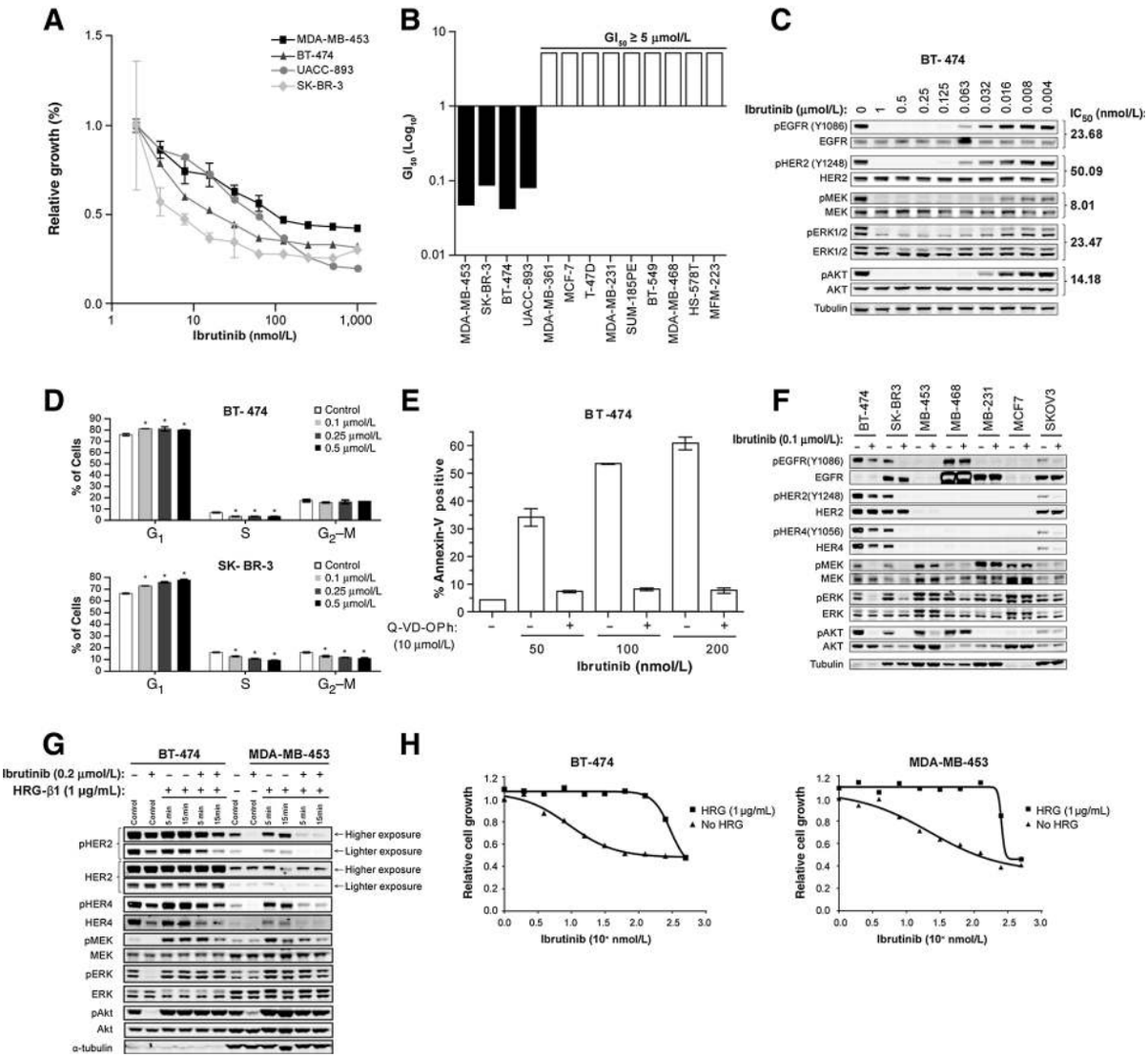

Figure 1.

Ibrutinib inhibited HER2-amplified breast cancer cell lines and key signaling pathways *in vitro*. **A,** A representative 72-hour proliferation assay for four HER2-amplified breast cancer cell lines. Cells were treated in triplicate in 96-well plates. Error bars, SD. IC_{50} for MDA-MB-453, BT-474, UACC-893, and SK-BR-3 was 185.67, 34.78, 62.25, and 2.90 nmol/L, respectively. **B,** Sensitivity to ibrutinib in 13 breast cancer lines (GI_{50}) with 72-hour proliferation assays. The data were selected from two or more repeated assays that had similar results for each line. $GI_{50} \geq 5$ μmol/L is much higher than what is achievable *in vivo* and is considered inactive to ibrutinib. **C,** Dose–response of EGFR, HER2, MEK, ERK1/2, and AKT phosphorylation to ibrutinib after 1.5 hours of treatment for BT-474 cells. IC_{50} was calculated from densitometric measurement on Western blots. **D,** Cell-cycle measurement for BT-474 and SK-BR-3 cells by flow cytometry. The cells were treated for 1 hour with ibrutinib, washed, and then continued in culture for 24 hours. Error bars, SD; *, statistically significant from control ($P < 0.05$ or 0.01). **E,** The percentage of Annexin-V positivity for BT-474 cells treated for 72 hours in 6-well plates in triplicate. Ibrutinib was used at indicated concentrations with and without caspase inhibitor Q-VD-OPh. **F,** The effect of ibrutinib on ERBB kinase signaling in multiple cell lines after 1 hour of treatment; 50,000 cells were loaded in each lane. **G,** Cells were serum starved overnight and treated with ibrutinib at 0.2 μmol/L for 30 minutes with heregulin-β1 (HRG) added at the last 5 or 15 minutes. Cells (8×10^4) were loaded per lane. With the presence of HRG, the inhibitory effect of ibrutinib was reduced. **H,** A 3-day proliferation assay with or without HRG. The anti-proliferation effect of ibrutinib was inhibited by HRG, which was reversed only at high concentration of ibrutinib.

Table 1. Inhibition of selected tyrosine kinases by ibrutinib and ERBB inhibitors

Compound	BTK IC_{50}, nmol/L	EGFR IC_{50}, nmol/L	HER2 IC_{50}, nmol/L	HER4 IC_{50}, nmol/L	ITK IC_{50}, nmol/L
Ibrutinib	0.381	1.81	12.1	1.0	77.9
Afatinib	>1,000	0.458	5.43	0.704	412
Neratinib	48.2	0.825	3.76	0.284	612
Lapatinib	>1,000	5.3	35.1	10.8	>1,000
Gefitinib	>1,000	2.26	161	23.7	>1,000
Dacomitinib	416	0.278	7.11	0.747	474

profound effects at both low and high dose levels (12 and 50 mg/kg/d), in a dose-dependent manner, with the higher dose eliciting 90% tumor suppression by AUC (Fig. 2C). Subsequent pharmacokinetic study revealed that drug exposure was much higher in SCID mice than in nude and NOD-SCID mice (Supplementary Fig. S4B). E_{max} model fitting showed a close relationship between drug exposure (AUC) and tumor inhibition (Fig. 2C). $EAUC_{50}$ (half-maximal AUC) for tumor growth inhibition was calculated to be 835 ng · h/mL, in line with an achievable level after the standard 560 mg per day clinical dosing for lymphoma and CLL patients (3).

We analyzed BT-474 tumors from the BALB/c nude mice model for changes in related intracellular signaling pathways by IHC and Western blot analysis. IHC revealed that phosphor-HER2 was significantly lower at 48 mg/kg after 1 hour of final dosing, although the reduction was not apparent 8 hours postdosing or at 16 mg/kg (Fig. 2D). However, a clear reduction of pAKT was seen at both dose levels at 1-hour postdosing and detected up to 8 hours for the high dosage (Fig. 2E). Similar results were seen for pERK (Supplementary Fig. S4C). The difference in IHC results between pHER2, and pAKT and pERK is likely due to the different kinetics of the components in signaling pathways. Western blots for pAKT showed similar but more dramatic changes than IHC results for both doses: maximal inhibition of pAKT was noted at 1-hour postdosing, with residual inhibition persisting for at least 8 hours (Fig. 2F and Supplementary Fig. S4D).

Analysis of the pharmacokinetic/pharmacodynamic relationship was conducted using Western blot pAKT results (1-hour postdosing) from two BT-474 xenograft studies as a pharmacodynamic marker and the AUC of ibrutinib in the plasma of corresponding animals as a pharmacokinetic indicator. Figure 2G shows that the plasma exposure of ibrutinib correlated with pAKT inhibition in the tumors. $EAUC_{50}$ (half-maximal effective AUC) for pAKT inhibition was calculated to be 534 ng · h/mL, which is similar to observed exposures in human subjects after 420 mg/day dosing (29).

BTK and ITK binding and inhibition by ibrutinib compared with other EGFR and HER2 inhibitors

Given the shared activity of ibrutinib and other ERBB kinase inhibitors described earlier and the sequence homologies around the conserved cysteine residue for TEC and ERBB family kinases, we also explored whether those ERBB inhibitors had detectable activity against BTK and ITK. As shown in Table 1, those ERBB inhibitors were not active or more than 100-fold less active toward BTK in biochemical assay with recombinant enzymes. As for the ITK activity, they are more than 5-fold less potent or inactive. In cellular assays using Mino cells, an MCL line, ibrutinib inhibited phosphorylation of BTK and downstream molecules while other ERBB inhibitors showed little or no inhibition at the concentration tested (Fig. 3A). Moreover, neither neratinib nor dacomitinib established irreversible binding to BTK after 1 hour of incubation, except for slight binding by neratinib at higher concentrations in an occupancy assay using PCI-33380, a fluorescently tagged ibrutinib, as a probe (Fig. 3B). In contrast, nearly complete occupancy was achieved by ibrutinib at concentrations as low as 15 nmol/L. Thus, ibrutinib's spectrum of activity against both TEC family and HER2/EGFR is distinctive compared with other ERBB TKIs studied.

Irreversibility of inhibition

To further characterize irreversible inhibition of ERBB tyrosine kinases by ibrutinib, we examined the effect of drug washout on signaling pathways by incubating cells with ibrutinib for periods of time, followed by washing steps to remove unbound drug. When ibrutinib was present throughout the incubation period, phosphorylation of ERBB kinases, as well as the downstream targets pAKT and pERK, was clearly inhibited at both concentrations tested (0.1 and 0.5 μmol/L; Fig. 4A and Supplementary Fig. S5A). When washed out after 15 minutes of incubation, ibrutinib at 0.5 μmol/L still inhibited pHER2 and the downstream targets. In contrast, there was much reduced impact on phosphorylation of these molecules when cells were incubated at 0.1 μmol/L for 15 minutes before washout. However, if cells were incubated for a longer period of time (2 hours) before washout, ibrutinib retained most of its inhibitory activity, even at 0.1 μmol/L (Fig. 4A and Supplementary Fig. S5A). In comparison, ibrutinib was resistant to washout after incubation for 15 minutes at 0.1 μmol/L when BTK is a target (Fig. 4B), indicating that ibrutinib establishes irreversible binding to BTK more rapidly than to HER2. Nonetheless, 1-hour exposure to 0.1, 0.25, or 0.5 μmol/L ibrutinib inhibited subsequent growth of BT-474 (Fig. 4C) and SK-BR-3 cells (Supplementary Fig. S5B) over 6 days and induced cell death (Fig. 4D).

We further evaluated the irreversible binding of ibrutinib to *ERBB* kinases in biochemical assays using recombinant proteins with BTK as a control. Ibrutinib was resistant to dialysis and maintained its activities against BTK, HER4, and EGFR after preincubation with these enzymes for 1 hour, while the activity of LCK, a Src family kinase that lacks a conserved active-site cysteine and therefore cannot form covalent binding with ibrutinib, was completely restored after dialysis (Fig. 4E). Recombinant HER2 enzyme was not stable in the course of dialysis and could not be tested in such assays. The potency of irreversible inhibition was further quantified by rapid dilution assay, as described in Materials and Methods. The plots for HER2 and corresponding apparent k_{obs}, which indicate the potency of irreversible inhibition, are shown in Fig. 4F. Ibrutinib had potency of irreversible inhibition comparable with afatinib and neratinib, although binding to BTK was substantially more potent (Supplementary Fig. S5C). For EGFR and HER4, the potency of irreversible binding by ibrutinib was higher than afatinib and lower than neratinib (Supplementary Fig. S5C for EGFR and Supplementary Fig. S5D for HER4).

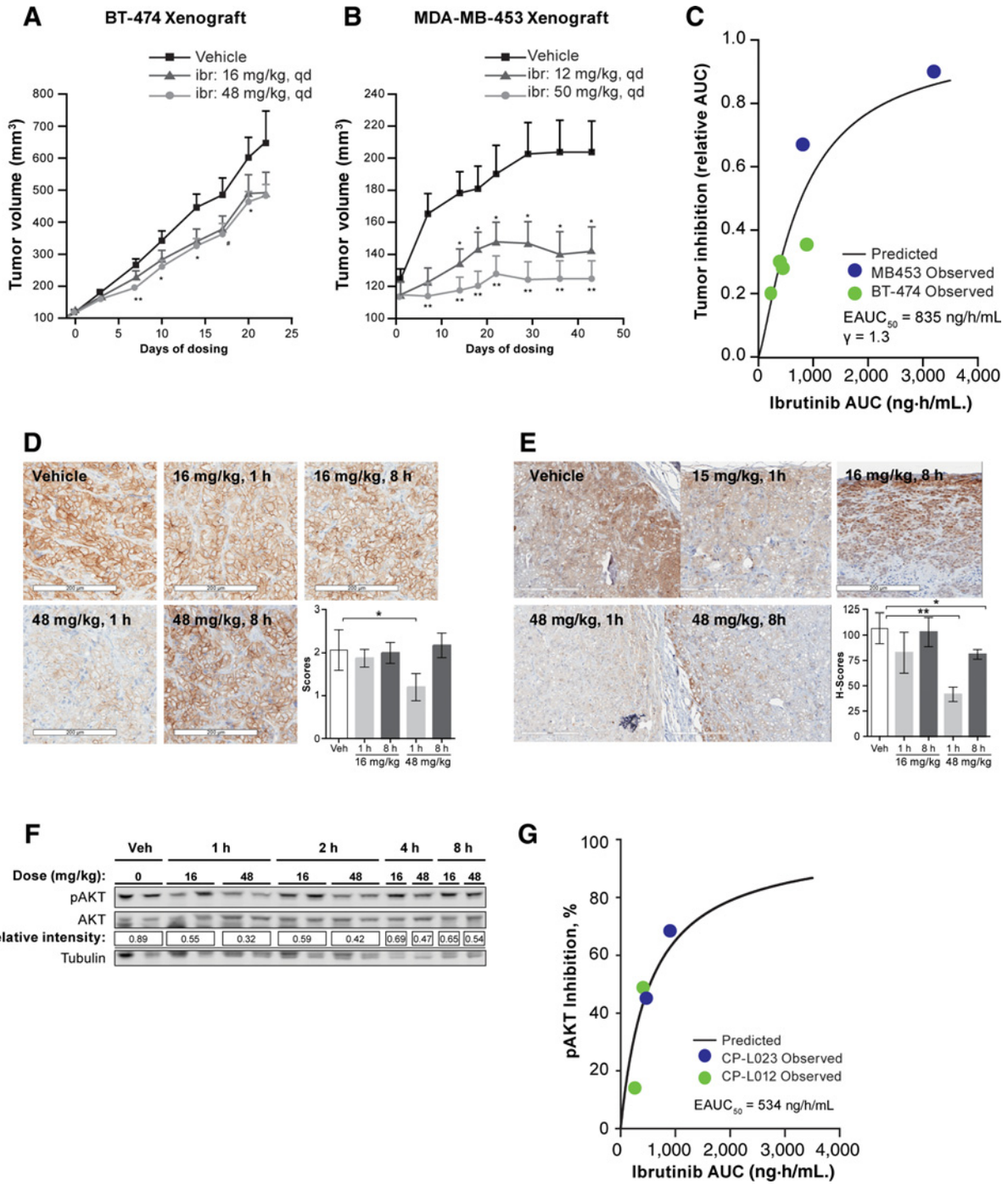

Figure 2.

Ibrutinib showed exposure-dependent inhibition of tumor growth and key signaling pathways in HER2-amplified breast cancer cell xenograft models. **A,** Inhibition of BT-474 xenograft growth in nude mice by ibrutinib administered at once-daily doses of 16 mg/kg (▲), or 48 mg/kg (●) compared with vehicle control (■). Significance for differences from control is indicated by *, $P < 0.05$ or **, $P < 0.01$); #, $P = 0.05$). **B,** Inhibition of MDA-MB-453 xenograft growth in SCID mice by ibrutinib administered at once-daily doses of 12 mg/kg (▲) or 50 mg/kg (●) compared with vehicle control (■). Statistical significance is as indicated in **A**. Error bars for **A** and **B** represent SE. **C,** E_{max} model fitting depicting relationship between drug exposure (AUC) and tumor inhibition. Data from two BT-474 xenograft studies and one MDA-MB-453 study were used for the fitting. **D,** Selected images for pHER2 staining from BT-474 tumors treated with ibrutinib at two time points and data analysis. *, $P < 0.05$. **E,** Selected images for pAKT staining from the same tumors; H-scores were calculated by multiplying the staining score and the percentage of the score in each image; *, $P < 0.05$ and **, $P < 0.01$. Error bars for **D** and **E** represent SD. **F,** Relative phosphorylation of AKT (pAKT/AKT) for harvested BT-474 tumors at different time points. For normalization, a ratio of pAKT/AKT was calculated for each band pair. Then all the bands were normalized to the first band of vehicle, which was assigned as 1.00. If there were two tumor samples for each treatment, an average value was given. **G,** E_{max} model fitting showing relationship between drug exposure (AUC) and relative AKT phosphorylation at 1-hour time point quantified with Western blots. Data were from two BT-474 xenograft studies.

Discussion

In this study, we have confirmed and extended the previously reported inhibitory activity of ibrutinib for ERBB family kinases. Consistent with its high enzymatic potency, ibrutinib exhibited significant cell growth inhibition, cell-cycle arrest, and caspase-dependent apoptosis of HER2-overexpressing breast cancer cell lines. Importantly, we have not found examples of HER2-negative breast cancer cell lines that are sensitive to ibrutinib in the course of several broad screenings. Sensitive cell lines had prominent basal AKT phosphorylation, as is known to be typical of HER2-driven cell lines (30, 31). Effects on cell growth in sensitive lines were accompanied by inhibition of activation of HER2 and other ERBB kinases, as well as downstream signaling through AKT and MEK-ERK, at concentrations comparable with those that suppressed cell proliferation (Figs. 1C and F, 4A, and Supplementary Fig. S3). The patterns of cellular inhibition were similar to what has been reported for other ERBB family kinase inhibitors (14, 21, 22). These observations suggested that HER2 inhibition was a major mechanism of ibrutinib's anticellular effects in the tested breast cancer lines. Although ibrutinib inhibited pEGFR in the cell lines tested and could also be a part of ibrutinib's mechanism of action (5), this receptor is not a known driver of the HER2-amplified breast lines studied. MDA-MB-453 had lower levels of pHER2 detectable by Western blot analysis but was nonetheless sensitive to ibrutinib. It behaved qualitatively similarly to BT-474 and SK-BR-3 with respect to inhibition of signal transduction pathways. The ERBB2 pathway was strongly activated in both MDA-MB-453 and BT-474 by the HER3- and HER4-specific ligand heregulin (Fig. 1G), and these cells became less sensitive to ibrutinib following activation by heregulin (Fig. 1H). This interplay between heregulin and ibrutinib further supported HER2 targeting as a major mechanism of ibrutinib's inhibition in these cell lines. MDA-MB-361, although a HER2-expressing cell line, also expresses hormonal receptors and harbors a PI3K-activating mutation, both of which could drive proliferation (23, 24). PI3K mutations in particular may lead to AKT activation and growth independent of HER2 (31). Consistently, Supplementary Fig. S1 suggested that PI3K is a main driver of the cells. Other mechanisms, such as HER3-dependent pathways that may modulate sensitivity to HER2 inhibition, were not specifically addressed in this study.

Irreversibility of the binding of ibrutinib to BTK is an advantageous attribute, enhancing specificity and facilitating a practical dosing schedule. The mere presence of a homologous cysteine in alternative targets does not, however, guarantee irreversibility of binding. In this study, ibrutinib was shown to irreversibly inhibit ERBB family kinases in both cellular and biochemical assays. Ibrutinib exhibited greater cellular growth inhibition than lapatinib, an approved EGFR/HER2 reversible inhibitor, and dacomitinib, an investigational irreversible pan-ERBB inhibitor. These comparisons were paralleled by results from biochemical assays of enzymatic activity. Although other irreversible inhibitors, such as neratinib and afatinib, had lower GI_{50} for cell growth than ibrutinib, they all showed comparable potency at concentrations above 50 nmol/L, which is easily achievable *in vivo*.

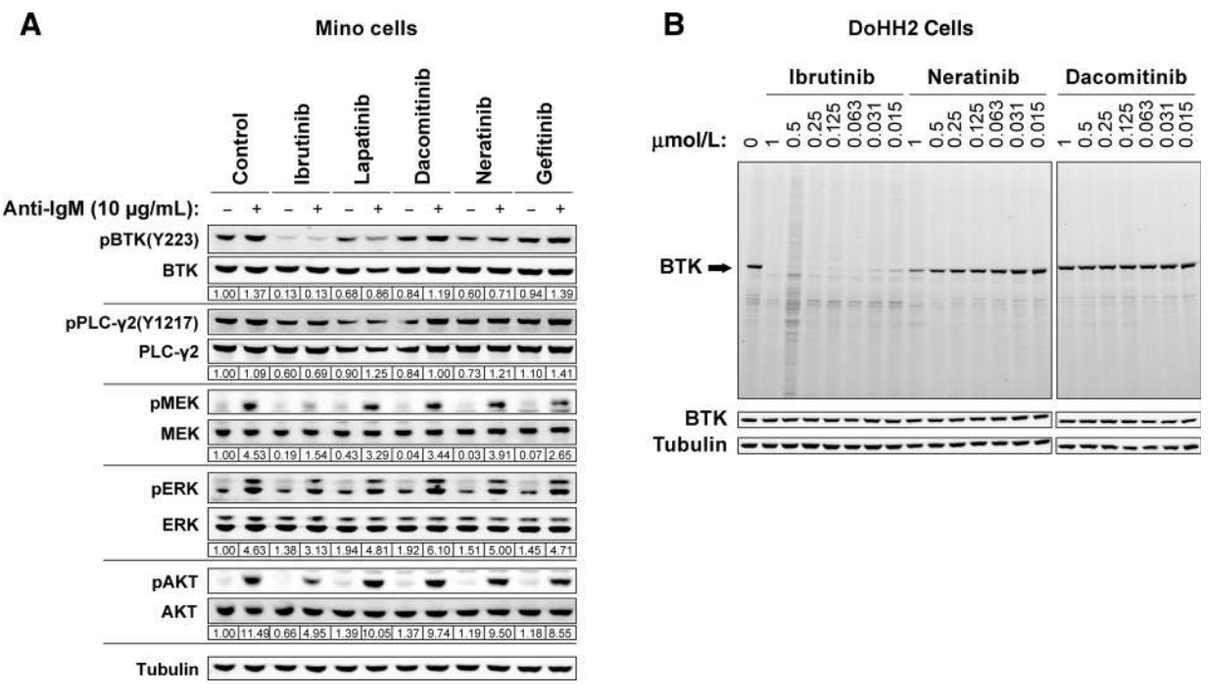

Figure 3.

Only ibrutinib was potent on inhibition of signal transduction and covalent BTK binding in B-lymphoma cells. **A,** Mino cells were pretreated with ibrutinib or other compounds for 1 hour and stimulated with anti-IgM antibody, $F(ab')_2$ for 5 minutes. Changes in protein phosphorylation were normalized to control cells without stimulation. **B,** Irreversible binding to BTK was tested with BTK occupancy assay. DOHH2 cells (10^6/mL) were treated with inhibitors for 1 hour, followed by 30-minute labeling with PCI-33380 (2 μmol/L). After electrophoresis of the cell lysates, the gel was scanned for fluorescently labeled bands. The expression of BTK was confirmed by Western blot analysis shown at the bottom.

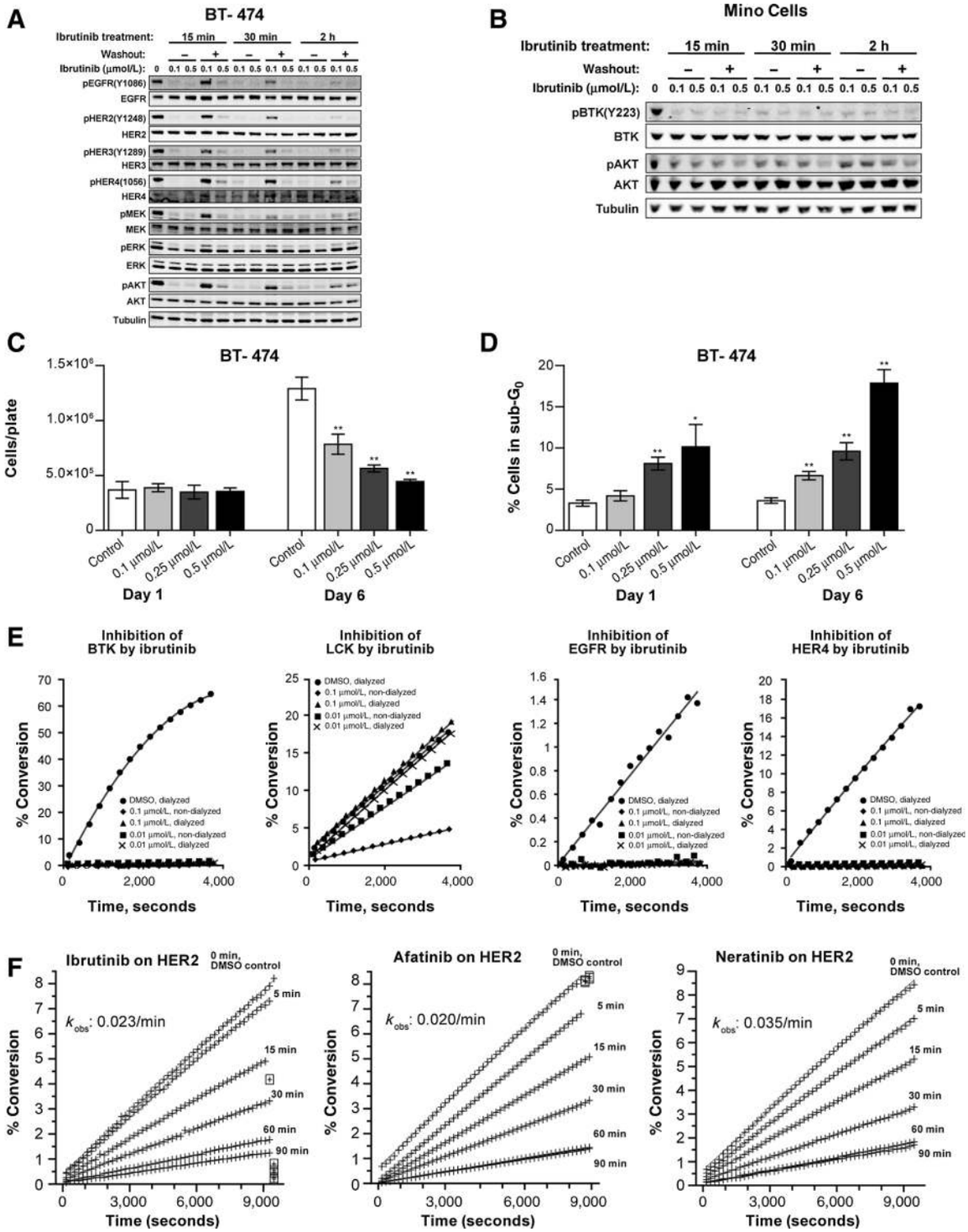

Figure 4.

Ibrutinib bound irreversibly to ERBB kinases and inhibited cell growth. **A,** BT-474 cells were treated with ibrutinib at 0.1 and 0.5 μmol/L for varied times before washed twice with fresh media or media with drug, as in the no-washout group. Cells were cultured for another 2 hours after washout before harvesting. **B,** Mino cells were treated similarly, as in **A. C,** the growth of BT-474 cells was still inhibited 6 days after original treatment with ibrutinib for 1 hour using wash-out steps. Cells were plated in 10-cm plate in triplicate, and washout was repeated twice. The cells were counted with a Coulter counter. **D,** Same set of cells as in **C** were measured for percentage of dead cells (sub G_0) with flow cytometry. Error bars for **C** and **D** were SD; *, $P < 0.05$ and **, $P < 0.01$. **E,** Dialysis assay to test irreversible binding by ibrutinib using recombinant enzymes. BTK was used as a positive control and LCK as a negative control. **F,** Indicates preincubation time for test compound and enzyme.

Although the evidence of *in vitro* enzymatic and cell growth effects was encouraging, we recognized the value of fully investigating ibrutinib activity *in vivo*, in two cell types and with pharmacokinetic and pharmacodynamic correlations. The most readily available and well- studied models of HER2$^+$ breast cancer are xenografts in mice that are immmunocompromised. Study of potential modulation of immune components by ibrutinib based on its activity for BTK and ITK was accordingly beyond the scope of the current study. Nonetheless, *in vivo* growth-inhibitory activity was noted in both BT-474 and MDA-MB-453 models. The apparently greater dose-related activity in the latter may have been caused by a difference in ibrutinib pharmacokinetics, most likely due to better bioavailability in the SCID mice used for MDA-MB-453 models, compared with nude or NOD-SCID mice used for BT-474 models. These differences were unexpected and previously unknown but will be helpful to us and other investigators in planning future studies. Inhibitory effects were relatively consistent between the two models on the basis of actual drug exposure (area under the plasma concentration–time curve, AUC) achieved (Fig. 2C). It is also possible, although, that differences in tumor kinetics could have complicated the comparison of these models, as rapid proliferation could counteract irreversibility of target inhibition by virtue of rapid synthesis of new and unaffected target.

The $EAUC_{50}$ for tumor inhibition derived from three xenograft studies was 835 ng · h/mL, and it was 534 ng · h/mL for pAKT inhibition measured on Western blots of excised tumors from BT-474 xenografts at 1 hour after dosing. These numbers are not far apart, with robust pAKT inhibition not surprisingly needed for tumor growth inhibition. Pharmacokinetics in humans has been well studied (3, 29), and our results in these tumor models compare well with the ranges noted clinically: in the phase I study, a MTD was not established, but the highest well-tolerated dose tested was 12.5 mg/kg/d, at which the mean steady state AUC was 1,445 ng · h/mL. It was 780 ng · h/mL in patients treated with 560 mg/d, the dose used for MCL, and 732 ng · h/mL in CLL patients treated with 420 mg/day. Results from a normal volunteer study were consistent with AUCs of 535–611 ng · h/mL observed following single 420-mg doses (29). Therefore, it is reasonable to anticipate clinical attainability of meaningful inhibition of similar, albeit generally more slow growing, human tumors. Ibrutinib was apparently less potent in these breast cancer models than in highly sensitive BTK-driven B-cell lymphoma models such as TMD8 (32) and OCI-Ly10 (33). In those studies, ibrutinib was effective at doses as low as 2–3 mg/kg; however, it was given intraperitoneally rather than orally, limiting direct comparability. In any case, it is clear that ibrutinib more potently binds to and inhibits BTK than HER2/EGFR.

Ibrutinib appears sufficiently potent as an irreversible HER2/EGFR TKI to possibly be active at clinically achievable doses and schedules. The potency of ibrutinib against HER2/EGFR kinases was not superior to that of some other irreversible inhibitors. However, ibrutinib might enhance its own direct activity against HER2/EGFR via modulation of accessory cells through inhibition of BTK and/or ITK. Recent findings (15, 16) highlighted intriguing activity of ibrutinib in immunotherapy models, attributed to T-cell–specific ITK. Genetic or pharmacologic inhibition of ITK in cells was shown to skew the balance of Th1 compared with Th2 cells. Corresponding shifts in the cytokine profile were observed in ibrutinib-treated CLL patients (15). Sagiv-Barfi and colleagues (16) demonstrated that ibrutinib in combination with anti–PD-L1 antibody provoked strong host T-cell–mediated antitumor activity against various tumor types, including triple-negative breast cancer, which led to high response rates and suppression of metastases. Others have reported ibrutinib modulation via BTK inhibition of myeloid-derived suppressor (17) or mast cells (18) in various solid tumor models. Our enzymatic and cellular assays indicated that the potential for such activities based on ITK and BTK inhibition were relatively unique for ibrutinib compared with other ERBB kinase family inhibitors studied. Recent clinical results have highlighted the potential importance of immune mechanisms in limiting efficacy of current HER2-targeting agents (34, 35).

In conclusion, we have presented evidence that ibrutinib, which has well known activity for TEC family kinases, also might serve as a clinically effective inhibitor of HER2-driven breast cancers. Ibrutinib's multifunctionality could be attractive in certain settings where both direct tumor inhibition and modulation of accessory cells would be desirable. Further investigation, both in the laboratory and in the clinic, is needed to test these hypotheses.

Disclosure of Potential Conflicts of Interest

J. Chen is a scientist at Pharmacyclics. J. Sukbuntherng has ownership interest (including patents) in AbbVie Shares (Global Blood Therapeutics Shares) and Portola Pharmaceuticals Shares. B.Y. Chang is employed at Pharmacyclics LLC, an AbbVie Company (clinical research). L. Elias is a senior fellow at Pharmacyclics, has ownership interest (including patents) in Abbvie, Inc., Gilead, Inc., Ziopharm, Inc., Exelexis, Inc., and Karyopharm, Inc., and is a consultant/advisory board member for Pharmacyclics LLC. All Pharmacyclics authors have patents and shares of Abbvie stock. No potential conflicts of interest were disclosed by the other author.

Authors' Contributions

Conception and design: J. Chen, T. Kinoshita, J. Sukbuntherng, B.Y. Chang, L. Elias

Development of methodology: J. Chen, B.Y. Chang, L. Elias

Acquisition of data (provided animals, acquired and managed patients, provided facilities, etc.): J. Chen, B.Y. Chang

Analysis and interpretation of data (e.g., statistical analysis, biostatistics, computational analysis): J. Chen, J. Sukbuntherng, L. Elias

Writing, review, and/or revision of the manuscript: J. Chen, T. Kinoshita, J. Sukbuntherng, B.Y. Chang, L. Elias

Administrative, technical, or material support (i.e., reporting or organizing data, constructing databases): L. Elias

Study supervision: T. Kinoshita, L. Elias

Acknowledgments

The authors would like to thank Patricia Thiemann and Michelle Cardima for *in vivo* pharmacology support, Purvi Jejurkar and Danielle Tonev for bioanalytical support, and Harisha Atluri for pharmacokinetic data analysis for the studies included in the article. We also would like to thank George Cole and Isaiah Dimery for critical review. Editorial support for the article was provided by Swati Ghatpande, PhD, with funding from Pharmacyclics LLC, an AbbVie Company.

Grant Support

The study was supported by Pharmacyclics LLC, an AbbVie Company.

The costs of publication of this article were defrayed in part by the payment of page charges. This article must therefore be hereby marked *advertisement* in accordance with 18 U.S.C. Section 1734 solely to indicate this fact.

Received November 18, 2015; revised August 25, 2016; accepted September 9, 2016; published OnlineFirst September 27, 2016.

References

1. Honigberg LA, Smith AM, Sirisawad M, Verner E, Loury D, Chang B, et al. The Bruton tyrosine kinase inhibitor PCI-32765 blocks B-cell activation and is efficacious in models of autoimmune disease and B-cell malignancy. Proc Natl Acad Sci U S A 2010;107:13075–80.
2. Burger JA, Buggy JJ. Emerging drug profiles: Bruton tyrosine kinase (BTK) inhibitor ibrutinib (PCI-32765). Leuk Lymphoma 2013;54:2385–91.
3. Advani RH, Buggy JJ, Sharman JP, Smith SM, Boyd TE, Grant G, et al. Bruton tyrosine kinase inhibitor ibrutinib (PCI-32765) has significant activity in patients with relapsed/refractory B-cell malignancies. J Clin Oncol 2013;31:88–94
4. Grabinski N, Ewald F. Ibrutinib (Imbruvica™) potently inhibits ErbB receptor phosphorylation and cell viability of ErbB2-positive breast cancer cells. Invest New Drugs 2014;32:1096–104.
5. Gao W, Wang M, Wang L, Lu H, Wu S, Dai B, et al. Selective antitumor activity of ibrutinib in EGFR-mutant non–small cell lung cancer cells. J Natl Cancer Inst 2014;106:dju204.
6. Ou SH. Second-generation irreversible epidermal growth factor receptor (EGFR) tyrosine kinase inhibitors (TKIs): a better mousetrap? A review of the clinical evidence. Crit Rev Oncol Hematol 2012;83:407–21.
7. Thiel A, Ristimäki A. Targeted therapy in gastric cancer. APMIS 2015;123: 365–72.
8. Cohen RB. Current challenges and clinical investigations of epidermal growth factor receptor (EGFR)- and ErbB family-targeted agents in the treatment of head and neck squamous cell carcinoma (HNSCC). Cancer Treat Rev 2014;40:567–77.
9. Mahipal A, Kothari N, Gupta S. Epidermal growth factor receptor inhibitors: coming of age. Cancer Control 2014;21:74–9.
10. Kwak E. The role of irreversible HER family inhibition in the treatment of patients with non-small cell lung cancer. Oncologist 2011;16: 1498–507.
11. Carmi C, Mor M, Petronini PG, Alfieri RR. Clinical perspectives for irreversible tyrosine kinase inhibitors in cancer. Biochem Pharmacol 2012;84:1388–99.
12. Arkin M, Moasser MM. HER-2-directed, small-molecule antagonists. Curr Opin Investig Drugs 2008;9:1264–76.
13. López-Tarruella S, Jerez Y, Márquez-Rodas I, Martín M. Neratinib (HKI-272) in the treatment of breast cancer. Future Oncol 2012;8:671–81.
14. Kalous O, Conklin D, Desai AJ, O'Brien NA, Ginther C, Anderson L, et al. Dacomitinib (PF-00299804), an irreversible Pan-HER inhibitor, inhibits proliferation of HER2-amplified breast cancer cell lines resistant to trastuzumab and lapatinib. Mol Cancer Ther 2012;11:1978–87.
15. Dubovsky JA, Beckwith KA, Natarajan G, Woyach JA, Jaglowski S, Zhong Y, et al. Ibrutinib is an irreversible molecular inhibitor of ITK driving a Th1-selective pressure in T lymphocytes. Blood 2013;122:2539–49.
16. Sagiv-Barfi I, Kohrt HE, Czerwinski DK, Ng PP, Chang BY, Levy R. Therapeutic antitumor immunity by checkpoint blockade is enhanced by ibrutinib, an inhibitor of both BTK and ITK. Proc Natl Acad Sci U S A 2015;112:E966–72.
17. Stiff A, Trikha P, Wesolowski R, Kendra K, Hsu V, Uppati S, et al. Myeloid-derived suppressor cells express Bruton's tyrosine kinase and can be depleted in tumor bearing hosts by ibrutinib treatment. Cancer Res 2016;76:2125–36.
18. Massó-Vallés D, Jauset T, Serrano E, Sodir NM, Pedersen K, Affara NI, et al. Ibrutinib exerts potent antifibrotic and antitumor activities in mouse models of pancreatic adenocarcinoma. Cancer Res 2015;75:1675–81.
19. Sharma SV, Haber DA, Settleman J. Cell line-based platforms to evaluate the therapeutic efficacy of candidate anticancer agents. Nat Rev Cancer 2010;10:241–53.
20. Holbeck SL, Collins JM, Doroshow JH. Analysis of Food and Drug Administration-approved anticancer agents in the NCI60 panel of human tumor cell lines. Mol Cancer Ther 2010;9:1451–60.
21. Kallioniemi OP, Kallioniemi A, Kurisu W, Thor A, Chen LC, Smith HS, et al. ERBB2 amplification in breast cancer analyzed by fluorescence in situ hybridization. Proc Natl Acad Sci U S A 1992;89:5321–5.
22. Szöllösi J, Balázs M, Feuerstein BG, Benz CC, Waldman FM. ERBB-2 (HER2/neu) gene copy number, p185HER-2 overexpression, and intratumor heterogeneity in human breast cancer. Cancer Res 1995;55:5400–7.
23. Wang YC, Morrison G, Gillihan R, Guo J, Ward RM, Fu X, et al. Different mechanisms for resistance to trastuzumab versus lapatinib in HER2-positive breast cancers—role of estrogen receptor and HER2 reactivation. Breast Cancer Res 2011;13:R121.
24. Mallon R, Feldberg LR, Lucas J, Chaudhary I, Dehnhardt C, Santos ED, et al. Antitumor efficacy of PKI-587, a highly potent dual PI3K/mTOR kinase inhibitor. Clin Cancer Res 2011;17:3193–203.
25. Kwei KA, Kung Y, Salari K, Holcomb IN, Pollack JR. Genomic instability in breast cancer: pathogenesis and clinical implications. Mol Oncol 2010;4:255–66.
26. Swanton C, Nicke B, Schuett M, Eklund AC, Ng C, Li Q, et al. ,Chromosomal instability determines taxane response. Proc Natl Acad Sci U S A 2009;106:8671–6.
27. Konecny GE, Pegram MD, Venkatesan N, Finn R, Yang G, Rahmeh M, et al. Activity of the dual kinase inhibitor lapatinib (GW572016) against HER-2-overexpressing and trastuzumab-treated breast cancer cells. Cancer Res 2006;66:1630–9.
28. Wood ER, Truesdale AT, McDonald OB, Yuan D, Hassell A, Dickerson SH, et al. A unique structure for epidermal growth factor receptor bound to GW572016 (Lapatinib): relationships among protein conformation, inhibitor off-rate, and receptor activity in tumor cells. Cancer Res 2004;64:6652–9.
29. de Jong J, Sukbuntherng J, Skee D, Murphy J, O'Brien S. Byrd JC, et al. The effect of food on the pharmacokinetics of oral ibrutinib in healthy participants and patients with chronic lymphocytic leukemia. Cancer Chemother Pharmacol 2015;75:907–16.
30. Moasser MM. The oncogene HER2: its signaling and transforming functions and its role in human cancer pathogenesis. Oncogene 2007;26: 6469–87.
31. She QB, Chandarlapaty S, Ye Q, Lobo J, Haskell KM, Leander KR, et al. Breast tumor cells with PI3K mutation or HER2 amplification are selectively addicted to Akt signaling. PLoS ONE 2008;3:e3065.
32. Ceribelli M, Kelly PN, Shaffer AL, Wright GW, Xiao W, Yang Y, et al. Blockade of oncogenic IκB kinase activity in diffuse large B-cell lymphoma by bromodomain and extraterminal domain protein inhibitors. Proc Natl Acad Sci U S A 2014;111:11365–70.
33. Yang Y, Shaffer AL III, Emre NC, Ceribelli M, Zhang M, Wright G, et al. Exploiting synthetic lethality for the therapy of ABC diffuse large B cell lymphoma. Cancer Cell 2012;21:723–37.
34. Carey LA, Berry DA, Cirrincione CT, Barry WT, Pitcher BN, Harris LN, et al. Molecular heterogeneity and response to neoadjuvant human epidermal growth factor receptor 2 targeting in CALGB 40601, a randomized phase III trial of paclitaxel plus trastuzumab with or without lapatinib. J Clin Oncol 2016;34:542–9
35. Salgado R, Denkert C, Campbell C, Savas P, Nucifero P, Aura C, et al. Tumor-infiltrating lymphocytes and associations with pathological complete response and event-free survival in HER2-positive early-stage breast cancer treated with lapatinib and trastuzumab: a secondary analysis of the NeoALTTO trial. JAMA Oncol 2015,1:448–54.